ORIGINAL RESEARCH

Reduced Aortic Distensibility is Associated With Higher Aorto-Carotid Wave Transmission and Central Aortic Systolic Pressure in Young Adults After Coarctation Repair

Remi Kowalski, MBBS; Melissa G. Y. Lee, MBBS; Lex W. Doyle, MD; Jeanie L. Y. Cheong, MD; Joseph J. Smolich, MBBS, PhD; Yves d'Udekem, MD, PhD; Jonathan P. Mynard, PhD; Michael M. H. Cheung, MBChB, FRCP, MD

***Background*—**The long-term prognosis of patients with repaired aortic coarctation is characterized by high rates of cardiovascular and cerebrovascular disease related to hypertension, the basis of which remains unclear. To define potential underlying mechanisms, we investigated aortic and carotid arterial biomechanics and wave dynamics, and determinants of aortic systolic blood pressure, in young adults after coarctation repair.

***Methods and Results*—**Aortic arch and carotid biomechanics, wave intensity and wave power, and central aortic blood pressure, were derived from echocardiography and brachial blood pressure in 43 young adults after coarctation repair and 42 controls. Coarctation subjects had higher brachial and central systolic blood pressure (P=0.04), while aortic compliance was lower and characteristic impedance (Z_c) higher. Although carotid intima-media thickness was higher (P<0.001), carotid biomechanics were no different. Carotid forward compression wave power was higher and was negatively correlated with aortic compliance (R^2=0.42, P<0.001) and distensibility (R^2=0.37, P=0.001) in coarctation subjects. Aortic wave power and wave reflection indices were no different in control and coarctation patients, but coarctation patients with elevated aortic Z_c had greater aorto-carotid transmission of forward compression wave power (P=0.006). Aortic distensibility was the only independent predictor of central aortic systolic blood pressure on multivariable analysis.

***Conclusions*—**Young adults following coarctation repair had a less compliant aorta, but no change in carotid biomechanics. Reduced aortic distensibility was related to greater transmission of aortic forward wave energy into the carotid artery and higher central aortic systolic blood pressure. These findings suggest that reduced aortic distensibility may contribute to later cardiovascular and cerebrovascular disease after coarctation repair. **(*J Am Heart Assoc*. 2019;8:e011411. DOI: 10.1161/JAHA.118.011411.)**

Key Words: coarctation of the aorta • echocardiography • high blood pressure • hypertension • vascular imaging • waves

More than 70 years after the development of surgical techniques to correct coarctation of the aorta, the morbidity and mortality of this patient group remains high compared with the general population.[1] Apart from local complications such as re-coarctation and aortic aneurysm formation, the long-term outlook for these patients is characterized by the early development of coronary artery and cerebrovascular disease,[2–4] with a recent large population-based study finding that survivors of coarctation repair suffered all-cause stroke on average almost 19 years earlier than the general population.[5] A significant risk factor for the development of cerebrovascular disease in adulthood is hypertension, which has been demonstrated in a high proportion of patients after coarctation surgery.[6–9] Clinical and echocardiographic measurements of arch re-obstruction are unable to delineate the patients at risk of hypertension.[7]

From the Heart Research Group, Murdoch Children's Research Institute, Parkville, Vic., Australia (R.K., M.G.Y.L., L.W.D., J.L.Y.C., J.J.S., Y.d'U., J.P.M., M.M.H.C.); Departments of Cardiology (R.K., M.M.H.C.), and Cardiac Surgery (Y.d'U.) Royal Children's Hospital, Parkville, Vic., Australia; Department of Newborn Services, Royal Women's Hospital, Parkville, Vic., Australia (L.W.D., J.L.Y.C.); Departments of Paediatrics (R.K., L.W.D., J.J.S., Y.d'U., J.P.M., M.M.H.C.), Obstetrics and Gynaecology, (L.W.D., J.L.Y.C.), and Biomedical Engineering (J.P.M.), University of Melbourne, Melbourne, Australia.

Correspondence to: Michael Cheung, MBChB, FRCP, MD, Department of Cardiology, Royal Children's Hospital, 50 Flemington Road, Parkville, Vic. 3052 Australia. E-mail: michael.cheung@rch.org.au

Received November 7, 2018; accepted January 31, 2019.

© 2019 The Authors. Published on behalf of the American Heart Association, Inc., by Wiley. This is an open access article under the terms of the Creative Commons Attribution-NonCommercial-NoDerivs License, which permits use and distribution in any medium, provided the original work is properly cited, the use is non-commercial and no modifications or adaptations are made.

Clinical Perspective

What Is New?

- This study presents a novel implementation of wave intensity and wave power analysis at 2 arterial sites in young adults following coarctation of the aorta repair.
- This has allowed for an assessment of wave energy distribution between these 2 sites.

What Are the Clinical Implications?

- This study has demonstrated elevated wave energy transmission into the carotid arteries of coarctation subjects compared with controls.
- This was related to reduced aortic distensibility in the coarctation subjects, and may be of relevance to the elevated risk of adult cerebrovascular disease in this group.

On the other hand, sensitive markers of early vascular dysfunction or remodeling, such as arterial distensibility and carotid intima-media thickness, and hemodynamic measures of aortic pulse wave propagation and reflection,[8,10–12] may provide valuable information on future cardiovascular risk in these patients.

One potential but as yet unstudied mechanism underlying an elevated stroke risk after coarctation repair is a greater transmission of wave energy from the aorta into cerebral arteries. This phenomenon is demonstrable in the presence of aortic coarctation, where it results from increased wave reflection at the site of coarctation, with resultant passage of greater reflected wave energy into major cephalic arteries.[13] Whether a similar phenomenon occurs late after repair of aortic coarctation, related to residual wave reflection from the coarctation site, is unknown.

Aside from a wave reflection mechanism, a higher aortic impedance could also lead to increased transmission of forward wave energy from the ascending aorta into cephalic arteries. In the context of normal aging, there is evidence that stiffening of the aorta outpaces stiffening of more peripheral large arteries (such as the carotid artery), thereby reducing or even reversing a normal stiffness gradient present in youth, which in turn can lead to increased transmission of the aortic forward wave into the carotid artery and higher pulsatile energy in cerebral arteries.[14–19] Whether an altered aorto-carotid stiffness gradient also occurs in young adults after coarctation repair is unknown, but would be of significant interest given findings in older adults that this is a predisposing factor for cerebral microvascular damage.[20]

If increased aorto-carotid wave transmission is evident in patients following coarctation repair, then an important allied question is whether factors contributing to this greater wave transmission also play a role in the elevated central blood pressure commonly present in these patients.[11,21] The importance of central arterial blood pressure in modulating cardiovascular risk is well established,[22] with evidence suggesting that this pressure may be a more sensitive marker of cardiovascular risk and end-organ damage than brachial artery blood pressure.[23] However, the demographic, cardiac (structural and functional) and vascular (structural and biomechanical) variables which predict an elevated central aortic systolic pressure after coarctation repair are yet to be defined.

Thus the aims of this study were to determine: (1) whether increased aorto-to-carotid artery wave transmission occurs after coarctation repair; (2) to what extent any such increased transmission is related to wave reflection within the aorta or to an alteration of the normal stiffness gradient between the aorta and carotid artery; and (3) whether the factor(s) underlying aorto-carotid artery wave transmission patterns are also predictive of an elevated central aortic systolic pressure after coarctation repair. To address these aims, echocardiographic wave intensity (WI) and wave power (WP) analyses of both the aortic arch and carotid artery were undertaken in young adults after coarctation repair and in a control group of similar age. WP analysis is similar to WI analysis,[24] but has the benefit that wave power is conserved at junctions, thereby allowing investigation of wave power distribution in the arterial network.[13,25] In addition, aortic and carotid biomechanics, carotid intima-media thickness (cIMT) and left ventricular (LV) anatomy and function were assessed by echocardiography.

Methods

Study Population

The study was approved by the Human Research Ethics Committee at the Royal Children's Hospital, with subjects who had undergone repair of aortic coarctation recruited from the cardiac surgical database of this institution. Normal birthweight (>2499 g) and term-born (≥37 weeks' gestational age) participants from the Victorian Infant Collaborative Study 1991 to 1992 cohort were used as controls.[26] All subjects gave informed consent to participate in the research.

A total of 43 coarctation and 42 control subjects attended the Royal Children's Hospital for anthropometric and blood pressure measurements, echocardiography, assessment of aortic and carotid vascular properties, and wave analyses. All measurements were performed in a single session by the same technologist. The data that support the findings of this study are available from the corresponding author upon reasonable request.

Anthropometric and Blood Pressure Measurements

Subjects were asked to abstain from alcohol, tobacco, and caffeine for at least 24 hours, and fasted for a minimum of 6 hours before their study appointment. Height was measured to the nearest 0.1 cm with shoes removed, and weight to the nearest 0.1 kg with digital scales. Body surface area (BSA) was calculated according to the formula of Dubois and Dubois,[27] with body mass index (BMI) defined as weight (kg)/height (m)^2. After 10 minutes of semi-recumbent rest in a quiet darkened room, brachial artery systolic (SBP), diastolic (DBP), mean (MBP) and pulse (PP) pressures were obtained from the right arm using a cuff

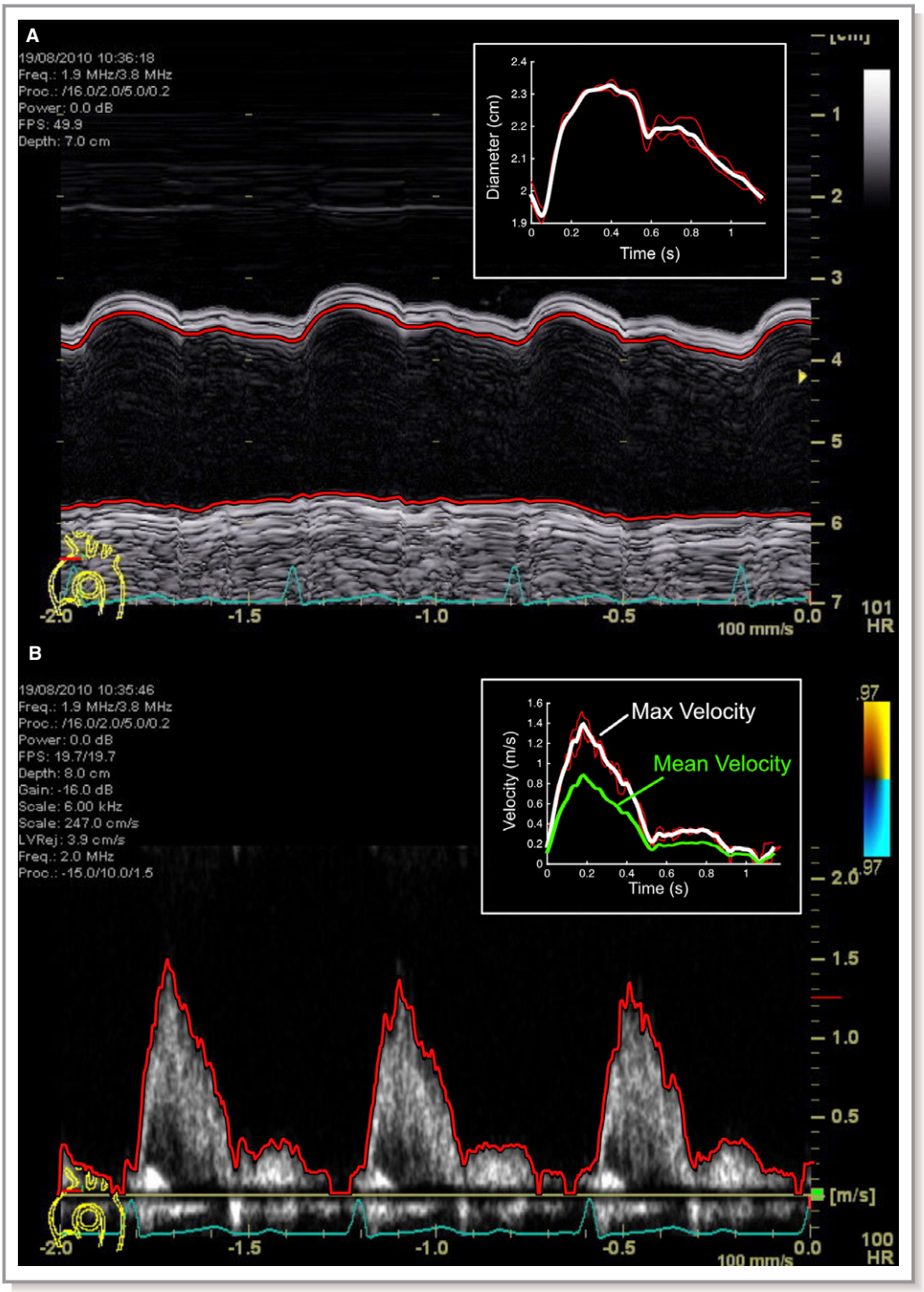

Figure 1. M-mode echocardiographic still-image of aortic arch diameter (**A**) and blood velocity (**B**), with automated edge segmentation and average beat files displayed in the inset boxes.

Table 1. Subject Demographics and Blood Pressure Variables

	Coarctation (n=43)	Control (n=42)	Unadjusted *P* Value	Difference in Means (±95% CI)*	*P* Value*
Age, y	25 (19, 29)	19 (18, 19)	<0.001†	…	…
Male	21 (48.8%)	15 (35.7%)	0.19‡	…	…
Height, cm	169.4±13.9	170.6±8.3	0.63	−6.6 (−2.6, −10.5)	0.001
Weight, kg	68.0 (57.3, 85.0)	65.5 (59.0, 73.5)	0.48†	0.6 (−6.6, 7.9)	0.87
BSA, m^2	1.81±0.27	1.79±0.21	0.51	−0.05 (−0.15, 0.05)	0.32
BMI, kg/m^2	23.7 (21.5, 27.1)	22.6 (20.8, 24.3)	0.22†	1.9 (−0.4, 4.1)	0.10
HR, beats per min	63±12	62±9	0.71	4 (0, 9)	0.07
Brachial SBP, mm Hg	131±12	117±11	<0.001	12 (7, 17)	<0.001
Brachial DBP, mm Hg	69 (64, 75)	66 (62, 69)	0.048†	1 (−3, 5)	0.54
Brachial PP, mm Hg	62 (52, 66)	51 (45, 56)	<0.001†	11 (6, 16)	<0.001
Central Aortic SBP, mm Hg	105 (101, 114)	100 (95, 109)	0.009†	6 (1, 11)	0.04
Central Aortic PP, mm Hg	38 (34, 49)	35 (31, 39)	0.07†	6 (1, 12)	0.02

Data are mean±SD. BSA indicates body surface area; BMI, body mass index; DBP, diastolic blood pressure; HR, heart rate; PP pulse pressure; SBP, systolic blood pressure.
*Data adjusted for age and sex.
†Median (25th, 75th percentiles) Mann–Whitney *U* test.
‡n (%), Chi-square test.

and digital oscillometric blood pressure monitor (HEM 705-CP, OMRON, Japan). Central aortic and carotid blood pressures were estimated by calibrating arterial diameter curves to brachial mean and diastolic blood pressure following the method of Quail et al.[28]

Echocardiography

Routine echocardiography was performed with patients in a semi-recumbent position using a GE Vivid 7 ultrasound machine (GE Medical Systems, Horten, Norway) with a

Table 2. Echocardiographic Data

	Coarctation (n=43)	Control (n=42)	Unadjusted *P* Value	Difference in Means (±95% CI)*	*P* Value*
LA z-score	1.00 (−0.21, 2.40)	0.74 (0.20, 1.30)	0.46†	0.42 (−0.33, 1.16)	0.27
AoRoot z-score	1.00 (0.05, 1.60)	0.20 (−0.21, 1.10)	0.07†	0.30 (−0.25, 0.85)	0.29
IVSd z-score	0.40 (−0.24, 1.10)	−0.11 (−0.40, 0.45)	0.02†	0.29 (−0.08, 0.67)	0.13
LV EDd z-score	0.49 (−0.34, 1.30)	0.20 (−0.26, 0.72)	0.45†	0.22 (−0.25, 0.70)	0.36
LV ESd z-score	−0.04 (−0.84, 0.82)	0.40 (0.08, 0.62)	0.10†	−0.30 (−0.78, 0.17)	0.21
LV PWd z-score	0.32 (−0.08, 0.94)	0.18 (−0.22, 0.72)	0.18†	0.11 (−0.31, 0.53)	0.62
LV mass, grams	145 (112, 209)	125 (108, 167)	0.03†	4 (−13, 21)	0.66
LV mass index, g/m^2	89 (72, 101)	75 (63, 85)	0.004†	4 (−3, 12)	0.23
FS, %	41 (37, 44)	36 (34, 40)	0.001†	3 (1, 6)	0.005
LVEF, %	68±4	66±4	0.06	1 (−1, 4)	0.18
Ascending aorta z-score	2.00±2.13	…	…		
Proximal transverse arch z-score	0.48±1.12	…	…		
Distal transverse arch z-score	0.41±1.21	…	…		
Isthmus z-score	0.30±1.29	…	…		
Descending aorta z-score	0.41±1.21	…	…		
Descending aorta V_{max}, m/s	2.06±0.51	…	…		

Data are mean±SD. AoRoot indicates aortic root; EDd, end-diastolic diameter; EF, ejection fraction; ESd, end-systolic diameter; FS, fractional shortening; IVSd, interventricular septal dimension; LA, left atrium; LV, left ventricle; PWd, posterior wall dimension; V_{max}, maximum Doppler velocity.
*Data adjusted for age and sex.
†Median (25th, 75th percentiles) Mann–Whitney *U* test.

Table 3. Arterial Biomechanical Properties

	Coarctation (n=30*/41†)	Control (n=28*/34†)	Unadjusted *P* Value	Difference in Means (±95% CI)‡	*P* Value‡
Aortic mean diameter, cm	2.17±0.39	2.36±0.22	0.02	−0.75 (−1.40, −0.09)	0.03
Carotid mean diameter, cm	0.66±0.07	0.64±0.06	0.11	0.02 (−0.02, 0.05)	0.40
Aortic ΔD, cm	0.36±0.10	0.43±0.10	0.01	−0.06 (−0.12, −0.01)	0.04
Carotid ΔD, cm	0.11 (0.09, 0.13)	0.09 (0.08, 0.11)	0.002§	0.02 (0.01, 0.03)	<0.001
Aortic strain	0.18±0.05	0.20±0.05	0.30	0.0 (−0.03, 0.02)	0.80
Carotid strain	0.18±0.04	0.16±0.03	0.01	0.03 (0.01, 0.05)	0.001
Aortic compliance, cm/mm Hg$\times 10^{-3}$	9.30±2.90	12.41±3.45	<0.001	−3.0 (−4.75, −1.27)	0.001
Carotid compliance, cm/mm Hg$\times 10^{-3}$	2.49 (2.24, 3.18)	2.70 (2.35, 3.34)	0.13§	−0.31 (−0.74, 0.11)	0.14
Aortic distensibility, 1/mm Hg$\times 10^{-3}$	4.71±1.67	5.66±1.73	0.04	−0.75 (−1.65, 0.15)	0.10
Carotid distensibility, 1/mm Hg$\times 10^{-3}$	4.19 (3.38, 5.07)	4.51 (3.77, 5.16)	0.13§	−0.54 (−1.26, 0.18)	0.14
cIMT, mm	0.56 (0.53, 0.62)	0.42 (0.41, 0.45)	<0.001§	0.13 (0.10, 0.16)	<0.001

Data are mean±SD. cIMT indicates carotid intima-media thickness; ΔD, change in aortic arch diameter during cardiac cycle.
*Aortic parameters.
†Carotid parameters.
‡Data adjusted for age and sex.
§Median (25th, 75th percentiles) Mann–Whitney *U* test.

5 MHz phased-array transducer for cardiac and aortic sonography, and a 10 MHz linear-array vascular probe for carotid artery imaging. M-mode echocardiography was performed according to American Society of Echocardiography guidelines[29] to determine aortic root, left atrial and left ventricular (LV) dimensions, which were normalized to the patient's body surface area by Z-scores.[30]

To assess LV systolic function, fractional shortening was calculated from M-mode and ejection fraction using the Simpson biplane method. LV mass (g) was calculated as $0.8\times(1.04[\text{LVEDd}+\text{IVSd}+\text{LVPWd}]^3-\text{LVEDd}^3)])+0.6$, where LVEDd is LV end-diastolic diameter, IVSd is end-diastolic interventricular septal thickness and LVPWd is LV end-diastolic posterior wall thickness, and normalized to body surface area to obtain LV mass index (LVMI).[31]

Carotid Intima-Media Thickness

Right common carotid artery (RCCA) imaging was performed 1 cm proximal to the carotid bulb with a high frequency linear probe (5–13 MHz), and cIMT measured at end-diastole[32] using wall-tracking software (EchoPAC, GE Vingmed Ultrasound, Norway). A minimum of 3 measurements were acquired and the mean of the readings used.

Aortic and Carotid Biomechanical Properties

Ten-beat M-mode cine-loops of (1) aortic arch diameter were recorded between the origins of the innominate and left common carotid arteries (Figure 1); and (2) RCCA diameter were recorded 2 cm proximal to the carotid bulb. After cropping and indexing to the fiducial electrocardiographic R-wave, semi-automated edge-detection, ensemble averaging, and smoothing of beats with a Savitzky-Golay[33] filter (second order, window width 7) were performed using customized software, with an effective sampling rate of 272 pixels/second. Following measurement of systolic and diastolic diameters, and calculation of their difference (ΔD), arterial strain was computed as (ΔD)/(diastolic diameter). Using estimated central blood pressure, arterial compliance was calculated as (ΔD)/(pulse pressure) and distensibility as (ΔD)/(diastolic diameter×pulse pressure).[34]

Aortic and Carotid Wave Analyses

Aortic arch and RCCA echocardiographic wave intensity (WI) were analyzed as previously described,[35] based on prior approaches used in peripheral arteries.[36–38] We also calculated the associated wave power (WP), using pressure and flow rather than pressure and velocity.[25] Using pulse-wave Doppler, a 10-beat cine-loop of aortic or carotid blood velocity was acquired (Figure 1), with cropping, edge-detection, averaging, and filtering as for arterial diameter. As central arterial distension and invasively-measured pressure waveforms correlate closely in systole,[39,40] the arterial diameter profile was converted to a pressure waveform via a two-point calibration using estimated central aortic or carotid arterial blood pressure.

Using a custom script written in Spike2 software (Cambridge Electronics Design, Cambridge, UK), velocity and pressure signals were ensemble-averaged. Mean velocity was then estimated from the maximum velocity (Doppler

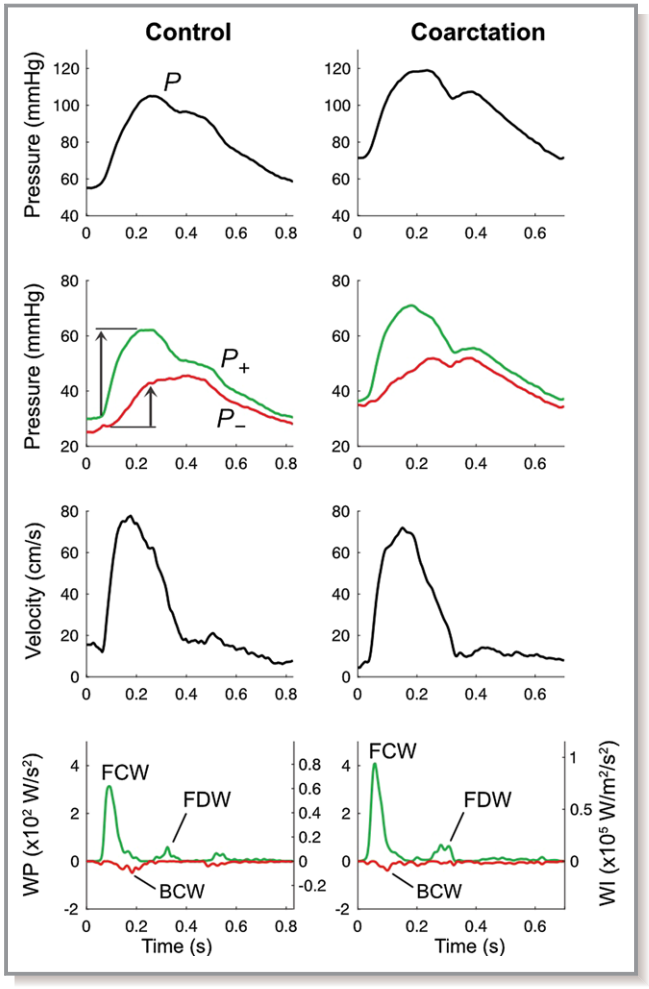

Figure 2. Example aortic pressure, velocity, wave power (WP) and wave intensity (WI) from control and coarctation participants. Top panel: aortic pressure waveform derived from averaged diameter distention waveforms. Second panel: aortic pressure separated into forward (P+) and backward (P−) components with arrows indicating wave-related pressure change (ΔP). Third panel: averaged aortic mean velocity waveforms. Lower panel: WP and WI separated into forward (green) and backward (red) components. BCW indicates backward compression wave; FCW, forward compression wave; FDW, forward decompression wave; WI, wave intensity; WP, wave power.

spectral envelope) using the scaling factors α and β described in our recent work.[41] Net WI was calculated as the instantaneous product of the rates of change in pressure and velocity,[42–44] and separated into forward and backward components using wave speed calculated with the ln(D)P loop method.[41] Blood flow was calculated as mean velocity multiplied by mean cross-sectional area, assuming a circular cross-section. WP was then obtained as the instantaneous product of the rates of change in pressure and flow, with separation into forward and backward components via use of characteristic impedance (Z_c, calculated as $\rho c/A$, where ρ=1.05 g/cm^3 is blood density, c is wave speed and A is vessel area).[25] For both WI and WP, "forward-running" and "backward-running" waves were defined as propagating away from and towards the ventricle respectively, while "compression" and "decompression" waves increased and decreased pressure, respectively.[24] Wave size was quantified by integrating over wave duration, resulting in the quantities of cumulative intensity and cumulative power. Forward and backward components of pressure were obtained by integrating pressure differentials, and wave-related pressure-change (ΔP) obtained as the pressure difference measured between the start and end of the wave.[45]

Statistical Analysis

Data were analyzed with SPSS (version 23, IBM Inc), with normality assessed using the Shapiro–Wilk test. Between-group data were compared with an independent Student *t* test for continuous normally-distributed data, a Mann–Whitney *U* test for non-normally distributed data, and Chi-square analysis for categorical variables, with $P<0.05$ considered statistically significant. Because there were demographic variations between coarctation repair and control subjects, differences between groups were also adjusted for age at assessment and sex, with findings based on the adjusted *P* value unless otherwise stated. The correlation between aortic stiffness variables and carotid forward wave power in each group, and the difference in these relationships, was assessed with linear regression. Box plots were constructed to compare the carotid to aortic forward wave power ratio of coarctation subjects having a high aortic characteristic impedance with those in control subjects, and in coarctation subjects with a normal impedance. Univariable associations of demographic, cardiac, and vascular data with central aortic SBP were assessed in the coarctation cohort, and variables with $P<0.10$ then entered into a multivariable linear regression using stepwise backward elimination. In the multivariable model, where independent variables were directly related to one another, only the variable with the higher correlation with the dependent variable was included.

Results

Subject Characteristics and Blood Pressure

Among the 43 coarctation subjects, the median (25th, 75th percentiles) age of surgical repair was 32 (8, 618) days, with 19 (44%) having a bicuspid aortic valve. Twenty subjects had a subclavian flap repair, 17 an end-to-end repair, and 6 subjects underwent multiple procedures or early re-do operations.

Compared with control subjects, the coarctation group was older, and shorter after adjusting for age and sex, but there were no differences in weight, body surface area, BMI, or

Table 4. Aortic Wave Analysis

	Coarctation (n=30)	Control (n=28)	Unadjusted *P* Value	Difference in Means (±95% CI)*	*P* Value*
c, m/s	3.44 (3.18, 4.00)	3.13 (2.90, 3.57)	0.03†	0.32 (−0.04, 0.69)	0.08
Z_c, g.cm^2/s	121 (95, 143)	89 (75, 98)	<0.001†	38 (17, 59)	0.001
Cumulative intensity, W/m^2/s×10^4					
FCW	2.26 (1.76, 3.74)	1.56 (1.36, 2.15)	0.01†	1.16 (0.31, 2.00)	0.008
BCW	−0.44 (−0.56, −0.33)	−0.42 (−0.48, −0.25)	0.37†	−0.23 (−0.43, −0.03)	0.02
FDW	0.49 (0.34, 1.27)	0.24 (0.18, 0.39)	<0.001†	0.44 (0.13, 0.75)	0.007
BCW:FCW cumulative intensity ratio	0.26±0.16	0.27±0.13	0.76	−0.01 (−0.10, 0.07)	0.77
Cumulative power, W/s					
FCW	7.29 (4.96, 18.46)	6.43 (5.01, 9.06)	0.49†	0.32 (−0.11, 0.74)	0.14
BCW	−1.52 (−2.69, −1.01)	−1.80 (−2.25, −1.02)	0.92†	−0.81 (−2.04, 0.41)	0.19
FDW	1.70 (1.01, 4.20)	1.03 (0.79, 1.54)	0.04†	0.17 (−0.01, 0.35)	0.06
BCW:FCW CP ratio	0.19 (0.14, 0.33)	0.27 (0.15, 0.34)	0.41†	−0.12 (−0.98, 0.65)	0.69
ΔP, mm Hg					
FCW	23.1 (20.7, 32.0)	20.5 (18.4, 23.7)	0.03†	5.28 (1.00, 9.55)	0.02
BCW	8.9 (7.7, 12.2)	8.4 (6.1, 9.5)	0.14†	2.44 (0.46, 4.42)	0.02
FDW	−10.9 (−14.7, −7.6)	−6.6 (−9.6, −5.2)	0.003†	−5.00 (−8.96, −1.03)	0.02
BCW:FCW ΔP ratio	0.45±0.16	0.44±0.14	0.71	0.01 (−0.08, 0.10)	0.81

Data are mean±SD. BCW indicates backward-running compression wave; c, local aortic wave speed; CP, cumulative power; FCW, initial systolic forward-running compression wave; FDW, late-systolic forward-running decompression wave; Z_c, characteristic impedance; ΔP, pressure change related to a given wave.
*Data adjusted for age and sex.
†Median (25th, 75th percentiles) Mann–Whitney *U* test.

heart rate between the groups (Table 1). The coarctation group had higher brachial artery SBP and PP, as well as higher central aortic SBP and PP.

Echocardiography

Left atrial, interventricular septal, LV posterior wall, end-diastolic and systolic z-scores were not statistically different. Although the unadjusted LV mass and mass index were greater in the coarctation group, these differences disappeared when the data were adjusted for the age and sex differences between groups. Both unadjusted and adjusted LV fractional shortening were elevated in the coarctation subjects (Table 2).

None of the coarctation patients had evidence of significant re-coarctation by echocardiography, with only 7 patients having a descending aortic velocity of >2.5 m/s (maximum 3.1 m/s), without any diastolic run-off.

Aortic Biomechanical Properties and Wave Analyses

Thirty coarctation and 28 control patients had sufficiently good image quality of the transverse aortic arch to perform biomechanical and wave analyses. Aortic ΔD and compliance were lower in coarctation patients, with a trend towards lower distensibility, while there was no difference in aortic strain (Table 3).

Wave analysis revealed 3 major wave types in the aortic arch (Figure 2): a pressure-increasing initial-systolic forward compression wave (FCW) related to impulsive LV ejection, an initial pressure-increasing backward compression wave (BCW) arising from vascular reflection of FCW, and a pressure-decreasing late-systolic forward decompression wave (FDW) related to LV relaxation.[24]

Aortic characteristic impedance (Z_c) was elevated in coarctation subjects compared with controls, with a trend towards higher aortic wave speed (Table 4). Coarctation subjects had greater aortic FCW cumulative intensity and ΔP, but cumulative power was not different because of a smaller aortic diameter in the coarctation group. There was a greater BCW cumulative intensity in coarctation subjects, with a greater ΔP, but no difference in BCW cumulative power; FDW cumulative intensity and ΔP were higher in the coarctation group with a trend towards greater FDW cumulative power. There was no difference in the wave reflection indices calculated as the ratio of BCW:FCW cumulative intensity, BCW:FCW cumulative power or BCW:FCW ΔP.

Table 5. Carotid Wave Analysis

	Coarctation (n=41)	Control (n=34)	Unadjusted *P* Value	Difference in Means (±95% CI)*	*P* Value*
c, m/s	3.71±0.50	3.49±0.45	0.05	0.19 (−0.05, 0.43)	0.11
Z_c, g.cm^2/s	1313±258	1315±295	0.98	22 (−118, 163)	0.75
Cumulative intensity, W/m^2/s×10^4					
FCW	3.18 (2.27, 4.11)	1.68 (1.28, 2.78)	<0.001†	1.80 (1.17, 2.44)	<0.001
BCW	−1.32 (−1.96, −0.89)	−0.84 (−1.23, −0.65)	0.002†	−0.74 (−1.10, −0.38)	<0.001
FDW	0.76 (0.56, 1.14)	0.33 (0.20, 0.58)	<0.001†	0.56 (0.36, 0.76)	<0.001
BCW:FCW cumulative intensity ratio	0.47±0.14	0.50±0.12	0.36	−0.04 (−0.11, 0.02)	0.21
Cumulative power, W/s					
FCW	0.99 (0.68, 1.50)	0.52 (0.41, 0.80)	<0.001†	0.67 (0.40, 0.95)	<0.001
BCW	−0.42 (−0.60, −0.28)	−0.26 (−0.41, −0.20)	<0.001†	−0.30 (−0.46, −0.13)	0.001
FDW	0.24 (0.17, 0.38)	0.10 (0.07, 0.17)	<0.001†	0.21 (0.13, 0.30)	<0.001
BCW:FCW wave power ratio	0.43±0.20	0.52±0.16	0.30	−0.04 (−0.10, 0.02)	0.18
ΔP, mm Hg					
FCW	24.3 (21.3, 28.6)	17.7 (16.1, 22.3)	<0.001†	7.1 (4.3, 9.9)	<0.001
BCW	15.0 (12.8, 20.5)	11.3 (9.7, 13.9)	<0.001†	4.5 (2.5, 6.6)	<0.001
FDW	−13.9 (−19.1, −11.3)	−9.4 (−14.0, −7.1)	<0.001†	−6.1 (−8.6, −3.6)	<0.001
BCW:FCW ΔP ratio	0.68±0.09	0.66±0.08	0.22	0.01 (−0.03, 0.06)	0.57

Data are mean±SD. BCW indicates backward-running compression wave; c, local aortic wave speed; CP, cumulative power; FCW, initial systolic forward-running compression wave; FDW, late-systolic forward-running decompression wave; Z_c, characteristic impedance; ΔP, pressure change related to a given wave.
*Data adjusted for age and sex.
†Median (25th, 75th percentiles) Mann–Whitney *U* test.

Carotid Artery Biomechanical Properties and Wave Analyses

Forty-one coarctation and 34 control patients had sufficiently good image quality of the RCCA to perform biomechanical and wave analyses. cIMT was significantly higher in coarctation patients (Table 3). In contrast to aortic data, the carotid ΔD and strain were higher in coarctation patients, but the compliance and distensibility were no different.

There were no differences in RCCA wave speed or Z_c between groups (Table 5). Compared with controls, the coarctation subjects had greater carotid FCW, BCW, and FDW cumulative intensities and associated ΔP. Unlike the aortic findings, the cumulative power of the FCW, BCW and FDW were all significantly higher in the coarctation group, but there were no differences in carotid wave reflection indices calculated by the ratio of BCW:FCW cumulative intensity, BCW:FCW cumulative power or BCW:FCW ΔP (Figure 3).

Aorta-to-Carotid Artery Wave Transmission

RCCA FCW cumulative power was correlated with aortic compliance, distensibility, and Z_c in coarctation subjects, but not controls (Figure 4). There was a significant difference between coarctation and control subjects for the relationship between RCCA FCW cumulative power and aortic compliance (interaction term P=0.005) and distensibility (interaction term P=0.02), but not for the aortic Z_c. In controls, RCCA FCW cumulative power was 9.2±4.5% of aortic FCW cumulative power. This percentage was higher (16.9±9.3%, P=0.006) in coarctation patients with elevated aortic Z_c, defined via the 90th percentile of the control group Z_c, but was not different (11.6±5.9%, P=0.4) in coarctation patients with normal aortic Z_c (Figure 5).

Predictors of Central Aortic Systolic Pressure

Significant univariable associations of subject demographic, echocardiographic, and aortic vascular variables with central aortic systolic pressure among coarctation subjects are presented in Table 6. Age and sex were not associated with central systolic pressure. On univariable analysis, after adjusting for age and sex, LV fractional shortening, aortic distensibility, wave speed, and compliance were significantly associated with central aortic systolic pressure. Repair type was also significant, with greater systolic pressure in those who had undergone an end-to-end anastomosis compared with

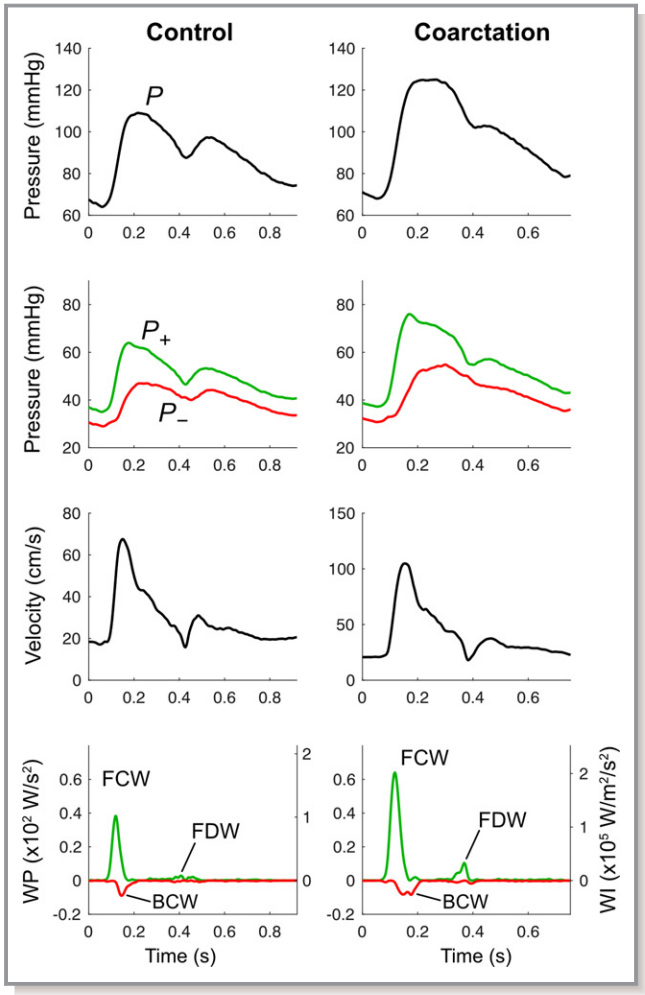

Figure 3. Example carotid pressure, velocity, wave power (WP) and wave intensity (WI) from control and coarctation participants. Top panel: carotid pressure waveform derived from averaged diameter distention wave forms. Second panel: carotid pressure separated into forward (P+) and backward (P−) components. Third panel: averaged carotid mean velocity waveforms. Lower panel: WP and WI separated into forward (green) and backward (red) components. BCW indicates backward compression wave; FCW, forward compression wave; FDW, forward decompression wave; WI, wave intensity; WP, wave power.

subclavian flap repair. In addition, there was a trend towards a relationship with subject height, but no significant relationships between central aortic pressure and indices of wave reflection, peak descending aortic velocity, or arch measurement z-scores.

On multivariable analysis, only aortic distensibility remained a significant predictor of central aortic systolic pressure, although a trend was evident towards a relationship with arch repair type.

Discussion

This is the first study to apply non-invasive arterial wave analyses (wave intensity and wave power) at 2 arterial sites in conjunction with central pressure assessment and standard echocardiographic and biomechanical analyses in young adults with repaired coarctation of the aorta. The main findings of our study were that these patients had: (1) evidence of increased transmission of wave power from the aorta into the carotid artery; (2) a functionally stiffer (ie, less distensible, less compliant, and higher Z_c) aorta but not carotid artery, despite a greater cIMT, resulting in a reduced stiffness gradient between these vessels which favored transmission of aortic wave energy into the carotid arteries; (3) no evidence of increased aortic or carotid arterial wave reflection; (4) a higher central aortic systolic pressure which was independently associated with aortic distensibility.

A major finding of the present study was that, following repair of aortic coarctation in infancy, young adults displayed evidence of increased transmission of wave energy from the aorta into carotid arteries. This conclusion was consistent with FCW and FDW cumulative power in the RCCA of the coarctation group being markedly higher than in the control group, whereas aortic FCW and FDW cumulative power were not statistically different between these groups. Note that a lack of difference in FCW and FDW power in the aorta of control and coarctation repair subjects contrasted with a greater aortic FCW and FDW *intensity* in the coarctation repair group, which was related to a smaller aortic diameter, and consequently a higher velocity acceleration (dU/dt) without an associated higher flow acceleration (dQ/dt).

Our data also suggested that biomechanical differences were present between the aorta and carotid artery following repair of aortic coarctation. Thus, reductions in distensibility, compliance and ΔD were evident in the aortic arch after coarctation repair, in keeping with previous studies.[8,11,12,46,47] Additionally, characteristic impedance was greater and local aortic wave speed tended to be higher after coarctation repair, which accords with a higher brachial-radial pulse wave velocity in a similarly aged cohort of coarctation patients.[48] Unlike pulse wave velocity, which refers to average wave speed over a length of vasculature, wave speed in our study was measured using a single-point method (ie, at the site of measurement),[24,41] which may be important given evidence of region-specific increases in stiffness within patients with coarctation.[46] By contrast, despite a higher cIMT, as observed in prior studies,[8,49] carotid diameter change and strain were increased, while characteristic impedance was no different to control subjects in the carotid artery after coarctation repair, suggesting that normal homeostatic remodeling of the carotid artery had taken place.

Taken together, the foregoing biomechanical findings, which are consistent with those of Sarkola et al,[8] suggest that there is a reduced aorto-carotid stiffness gradient in young adults with repaired aortic coarctation. While this

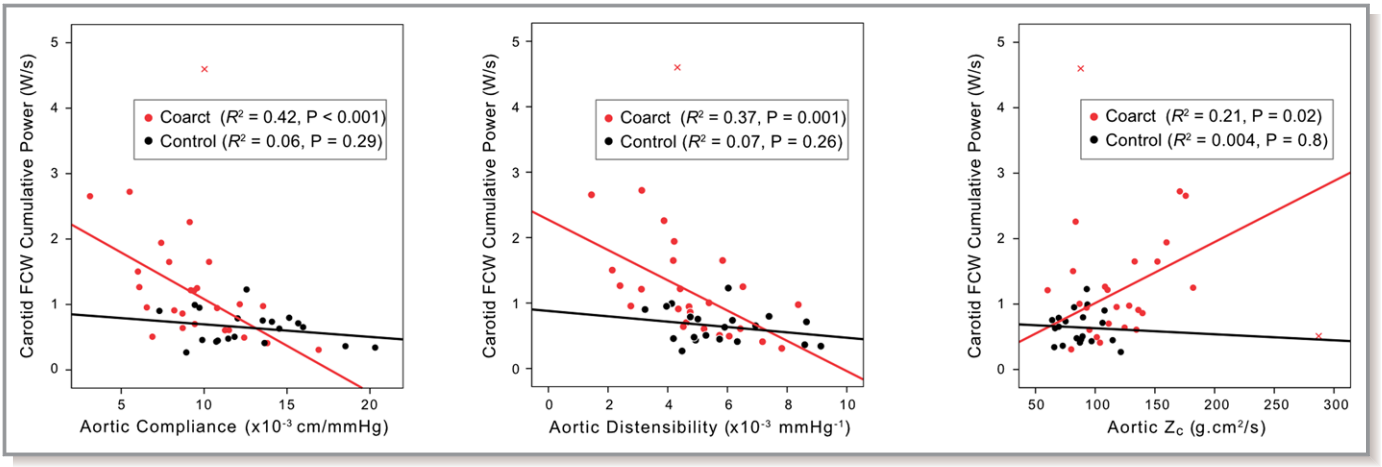

Figure 4. Correlation of carotid arterial FCW cumulative wave power with aortic compliance, distensibility, and characteristic impedance (Z_c) using pooled data from control and coarctation groups. Red crosses indicate outliers that were not included in the regression analysis. FCW indicates forward compression wave.

conclusion resembles that reached by Paini et al, in an elderly group of hypertensive subjects without coarctation,[14] it remains unclear whether this situation in coarctation patients results from more rapid stiffening of the aorta relative to the carotid artery, or from residual abnormalities in aortic size and distensibility that remain after surgery in infancy. Regardless of the underlying mechanism, however, the correlation between carotid arterial FCW power and aortic distensibility, compliance, and characteristic impedance (Figures 4 and 5) strongly suggested that this reduced stiffness gradient between the aorta and carotid artery contributed to elevated transmission of aortic forward wave energy towards the brain after coarctation repair.

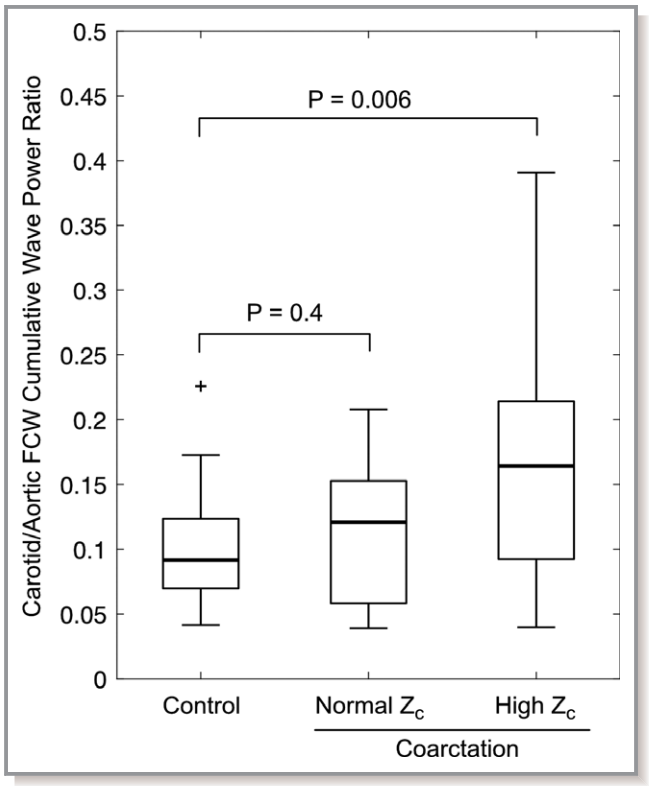

Figure 5. Box plots of the carotid/aortic FCW cumulative power ratio in controls and coarctation patients with normal and high aortic characteristic impedance (Z_c), where high Z_c was defined as >90th percentile of the control group. FCW indicates forward compression wave.

Somewhat unexpectedly, the degree of aortic wave reflection after coarctation repair, calculated using either the ratio of changes in pressure related to BCW and FCW, or the cumulative intensity or wave power BCW-to-FCW ratios, was not different to that of control subjects in our study. In turn, this finding indicated that, unlike the situation occurring in the presence of an overt aortic coarctation,[13] increased aortic wave reflection was not a mechanism that contributed to greater passage of forward wave energy from the aorta into major cephalic arteries following coarctation repair. Nevertheless, although not seen in our cohort, such a mechanism may play a role in patients exhibiting significant wave reflection from the repair site arising as a result of residual narrowing and/or stiffening.[50,51]

The lack of elevated aortic wave reflection in our study differs from several previous studies. Murakami et al[10] reported increased wave reflection in children assessed during cardiac catheterization after coarctation repair, based on an elevated augmentation index. On the other hand, Swan et al[52] reported no difference in augmentation index in normotensive adults after coarctation repair. However, augmentation index may not be a reliable index of wave reflection per se, since it has a major dependence on both aortic wave, speed, and forward wave amplitude.[53–56] Indeed, the time to inflection point on the aortic pressure trace was reduced by half in Murakami et al,[10] suggesting a substantially higher

Table 6. Significant Uni- and Multivariable Relationships of Demographic and Vascular Variables With Central Aortic Systolic Pressure Adjusted for Age and Sex Among Coarctation Subjects (n=28)

	Univariable			Multivariable	
	Regression Coefficient (95% CI)	% Variance Explained	*P* Value	Regression Coefficient (95% CI)	*P* Value
Height, cm	0.30 (−0.06, 0.67)	17.1	0.10		
Fractional Shortening, %	0.58 (0.01, 1.15)	7.2	0.05		
Aortic distensibility, 1/mm Hg$\times 10^{-3}$	−4.07 (−6.46, −1.68)	37.7	0.002	−3.52 (−6.62, −0.42)	0.03
Aortic compliance, cm/mm Hg$\times 10^{-3}$	−1.74 (−3.29, −0.19)	21.9	0.03		
Aortic c, m/s	8.59 (3.64, 13.54)	39.0	0.002		
Repair (1=subclavian flap; 2=end-end)	9.0 (2.7, 15.3)	17.6	0.007	5.98 (−0.17, 12.12)	0.06

c indicates wave speed.

aortic wave speed in the coarctation group. Whether this accounts for the increased augmentation index rather than increased reflection magnitude would need to be clarified via wave separation analysis, which specifically reveals forward and backward waves.

In a recent magnetic resonance imaging study of ascending aortic wave intensity by Quail et al,[11] wave reflection quantified as the ratio of backward area to forward area waveforms was higher in young adults after coarctation repair compared with controls (0.91 versus 0.88). Although not in the original publication, the BCW:FCW cumulative intensity ratio was also higher in the coarctation group (0.16 versus 0.08, personal communication with the authors of Quail et al[11]). The reasons why these findings differ from those of our study is unclear, but could be related to factors such as differing imaging modalities (magnetic resonance imaging versus ultrasound) and acquisition locations (ascending aorta versus transverse aortic arch), or differences in patient characteristics given that, unlike in our study, subjects after coarctation repair in Quail et al[11] had a higher LV mass index and a similar aortic FCW intensity to controls.

The elevated brachial and central blood pressure indices in the present study are consistent with our previous report,[6] and similar to the elevation in systolic pressure after coarctation repair reported by other investigators.[7] We have further extended these observations by demonstrating that, amongst demographic, cardiac, and vascular variables, lower aortic distensibility was the only independent predictor of central aortic systolic pressure. Importantly, neither echocardiographic measures of aortic arch size and descending aortic velocity nor wave reflection indices were predictive of central aortic SBP on either univariable or multivariable analysis. These results accord with previous authors who have demonstrated high proportions of hypertension in patients after coarctation repair in the absence of obvious aortic re-obstruction.[7,9]

Despite elevated brachial and central systolic blood pressures compared with controls, subjects after coarctation repair had an elevated LV fractional shortening without LV dilation, similar to the findings of prior studies.[57–61] However, while our conclusion that LVMI was not elevated following surgical repair of coarctation accords with the observation of Sarkola,[8] it differs from the increased LVMI reported in other studies.[11,47,61] Factors that may have contributed to this difference include: (1) our use of echocardiography to obtain LVMI, rather than magnetic resonance imaging,[11,47]; and (2) our adjustment of LVMI data for age and sex, noting that unadjusted LVMI was elevated in post-coarctation repair patients (Table 2).

Limitations

Two study limitations require comment. First, adequate visualization of both the carotid artery and transverse aortic arch walls was not possible in all patients. The application of another imaging modality such as cardiac magnetic resonance imaging to this cohort could overcome limitations related to poor aortic arch imaging windows. Second, our cohort was not sufficiently powered to investigate biomechanical differences between surgical repair techniques, but this would be an important avenue of further study given the trend for an association of surgical technique with central aortic systolic pressure in our multivariable analysis.

Conclusions

In this study, young adults following coarctation repair had increased aorto-carotid wave transmission compared with controls, as demonstrated by significantly elevated carotid arterial, but not aortic, forward wave power. This phenomenon was accompanied by a reduction of the normal aorto-carotid stiffness gradient, higher aortic characteristic impedance, and lower aortic arch compliance, but no evidence of parallel changes in the corresponding carotid values. Lower aortic

distensibility was associated with central aortic SBP on multivariable analysis in the coarctation group, and correlated with increased carotid wave transmission. Despite elevated brachial and central aortic systolic pressures, there was no evidence of increased aortic wave reflection in the coarctation group. The increase in aorto-carotid transmission of wave energy following surgical repair of aortic coarctation may contribute to the high rates of cerebrovascular disease in this group.[5]

Acknowledgments

We thank Jane Koleff for acquisition of echocardiographic and vascular function data. The following members of the Victorian Infant Study Group were involved in data collection on the controls for this study. Convenor: Jeanie Cheong (Premature Infant Follow-up Program at the Royal Women's Hospital). Collaborators (in alphabetical order): Elizabeth Carse (Monash Medical Centre), Lex W. Doyle (Premature Infant Follow-up Program at the Royal Women's Hospital, Departments of Obstetrics and Gynaecology and Paediatrics, University of Melbourne, and Murdoch Childrens Research Institute), Marie Hayes (Monash Medical Centre), Marion McDonald (Premature Infant Follow-up Program at the Royal Women's Hospital), Gillian Opie (Mercy Hospital for Women), Gehan Roberts (Premature Infant Follow-up Program at the Royal Women's Hospital and Paediatrics, University of Melbourne and Royal Children's Hospital, Melbourne, Australia), Andrew Watkins (Mercy Hospital for Women).

Sources of Funding

This work was supported by a National Health and Medical Research Council (NHMRC) Postgraduate Scholarship to Dr Kowalski, Heart Kids Grant-in-aid G005, NHMRC Project grant 491246, Centre of Research Excellence 1060733, the Victorian Government's Operational Infrastructure Support Program, and RCH 1000 of the Royal Children's Hospital Foundation. A/Prof d'Udekem is a NHMRC Clinician Practitioner Fellow (1082186). Dr Lee is supported by a Health Professional Scholarship from the National Heart Foundation of Australia (NHF, 100681). Dr Mynard is supported by a co-funded Career Development Fellowship/Future Leader Fellowship from the NHMRC and NHF. Dr Cheong has an NHMRC Career Development Fellowship (1141354).

Disclosures

Dr Mynard is a consultant for the Brain Protection Company (this work was not conducted as part of this consultancy). The remaining authors have no disclosures to report.

References

1. Celermajer DS, Greaves K. Survivors of coarctation repair: fixed but not cured. *Heart*. 2002;88:113–114.
2. Cohen M, Fuster V, Steele PM, Driscoll D, McGoon DC. Coarctation of the aorta. Long-term follow-up and prediction of outcome after surgical correction. *Circulation*. 1989;80:840–845.
3. Wu M-W, Chen H-C, Kao F-Y, Huang S-K. Risk of systemic hypertension and cerebrovascular accident in patients with aortic coarctation aged <60 years (from a national database study). *Am J Cardiol*. 2015;116:779–784.
4. Connolly HM, Huston J, Brown RD, Warnes CA, Ammash NM, Tajik AJ. Intracranial aneurysms in patients with coarctation of the aorta: a prospective magnetic resonance angiographic study of 100 patients. *Mayo Clin Proc*. 2011;78:1491–1499.
5. Pickard SS, Gauvreau K, Gurvitz M, Gagne JJ, Opotowsky AR, Jenkins KJ, Prakash A. Stroke in adults with coarctation of the aorta: a national population-based study. *J Am Heart Assoc*. 2018;7:e009072–e009079. DOI: 10.1161/JAHA.118.009072.
6. Lee MGY, Kowalski R, Galati JC, Cheung MMH, Jones B, Koleff J, d'Udekem Y. Twenty-four-hour ambulatory blood pressure monitoring detects a high prevalence of hypertension late after coarctation repair in patients with hypoplastic arches. *J Thorac Cardiovasc Surg*. 2012;144:1110–1118.
7. Hager A, Kanz S, Kaemmerer H, Schreiber C, Hess J. Coarctation Long-term Assessment (COALA): significance of arterial hypertension in a cohort of 404 patients up to 27 years after surgical repair of isolated coarctation of the aorta, even in the absence of restenosis and prosthetic material. *J Thorac Cardiovasc Surg*. 2007;134:738–745.e2.
8. Sarkola T, Redington AN, Slorach C, Hui W, Bradley T, Jaeggi E. Assessment of vascular phenotype using a novel very-high-resolution ultrasound technique in adolescents after aortic coarctation repair and/or stent implantation: relationship to central haemodynamics and left ventricular mass. *Heart*. 2011;97:1788–1793.
9. O'Sullivan JJ, Derrick G, Darnell R. Prevalence of hypertension in children after early repair of coarctation of the aorta: a cohort study using casual and 24 hour blood pressure measurement. *Heart*. 2002;88:163–166.
10. Murakami T, Takeda A. Enhanced aortic pressure wave reflection in patients after repair of aortic coarctation. *Ann Thorac Surg*. 2005;80:995–999.
11. Quail MA, Short R, Pandya B, Steeden JA, Khushnood A, Taylor AM, Segers P, Muthurangu V. Abnormal wave reflections and left ventricular hypertrophy late after coarctation of the aorta repair. *Hypertension*. 2017;69:501–509.
12. Brili S, Dernellis J, Aggeli C, Pitsavos C, Hatzos C, Stefanadis C, Toutouzas P. Aortic elastic properties in patients with repaired coarctation of aorta. *Am J Cardiol*. 1998;82:1140–1143.A10.
13. Mynard JP, Kowalski R, Cheung MMH, Smolich JJ. Beyond the aorta: partial transmission of reflected waves from aortic coarctation into supra-aortic branches modulates cerebral hemodynamics and left ventricular load. *Biomech Model Mechanobiol*. 2016;16:635–650.
14. Paini A, Boutouyrie P, Calvet D, Tropeano A-I, Laloux B, Laurent S. Carotid and aortic stiffness: determinants of discrepancies. *Hypertension*. 2006;47:371–376.
15. O'Rourke MF, Staessen JA, Vlachopoulos C, Duprez D, Plante GE. Clinical applications of arterial stiffness; definitions and reference values. *Am J Hypertens*. 2002;15:426–444.
16. Boutouyrie P, Laurent S, Benetos A, Girerd XJ, Hoeks AP, Safar ME. Opposing effects of ageing on distal and proximal large arteries in hypertensives. *J Hypertens Suppl*. 1992;10:S87–S91.
17. O'Rourke MF, Nichols WW. Aortic diameter, aortic stiffness, and wave reflection increase with age and isolated systolic hypertension. *Hypertension*. 2005;45:652–658.
18. Safar ME, Levy BI, Struijker-Boudier H. Current perspectives on arterial stiffness and pulse pressure in hypertension and cardiovascular diseases. *Circulation*. 2003;107:2864–2869.
19. Mitchell GF, Parise H, Benjamin EJ, Larson MG, Keyes MJ, Vita JA, Vasan RS, Levy D. Changes in arterial stiffness and wave reflection with advancing age in healthy men and women: the Framingham Heart Study. *Hypertension*. 2004;43:1239–1245.
20. Mitchell GF, van Buchem MA, Sigurdsson S, Gotal JD, Jonsdottir MK, Kjartansson Ó, Garcia M, Aspelund T, Harris TB, Gudnason V, Launer LJ. Arterial stiffness, pressure and flow pulsatility and brain structure and function: the Age, Gene/Environment Susceptibility—Reykjavik Study. *Brain*. 2011;134:3398–3407.
21. Szczepaniak-Chichel L, Trojnarska O, Mizia-Stec K, Gabriel M, Grajek S, Gąsior Z, Kramer L, Tykarski A. Augmentation of central arterial pressure in adult patients after coarctation repair. *Blood Press Monit*. 2011;16:22–28.
22. Williams B, Lacy PS, Thom SM, Cruickshank K, Stanton A, Collier D, Hughes AD, Thurston H, O'Rourke M; CAFE Investigators, Anglo-Scandinavian Cardiac Outcomes Trial Investigators, CAFE Steering Committee and Writing Committee. Differential impact of blood pressure-lowering drugs on central aortic pressure and clinical outcomes: principal results of the Conduit Artery Function Evaluation (CAFE) study. *Circulation*. 2006;113:1213–1225.
23. Kollias A, Lagou S, Zeniodi ME, Boubouchairopoulou N, Stergiou GS. Association of central versus brachial blood pressure with target-organ

damage: systematic review and meta-analysis. *Hypertension*. 2016;67:183–190.

24. Parker KH. An introduction to wave intensity analysis. *Med Biol Eng Comput*. 2009;47:175–188.
25. Mynard JP, Smolich JJ. Novel wave power analysis linking pressure-flow waves, wave potential, and the forward and backward components of hydraulic power. *Am J Physiol Heart Circ Physiol*. 2016;310:H1026–H1038.
26. Kowalski RR, Beare R, Doyle LW, Smolich JJ, Cheung MMH; Victorian Infant Collaborative Study Group. Elevated blood pressure with reduced left ventricular and aortic dimensions in adolescents born extremely preterm. *J Pediatr*. 2016;172:75–80.e2.
27. Du Bois D, Du Bois EF. Clinical calorimetry: tenth paper a formula to estimate the approximate surface area if height and weight be known. *Arch Inter Med*. 1916;17:863.
28. Quail MA, Steeden JA, Knight D, Segers P, Taylor AM, Muthurangu V. Development and validation of a novel method to derive central aortic systolic pressure from the MR aortic distension curve. *J Magn Reson Imaging*. 2013;40:1064–1070.
29. Lopez L, Colan SD, Frommelt PC, Ensing GJ, Kendall K, Younoszai AK, Lai WW, Geva T. Recommendations for quantification methods during the performance of a pediatric echocardiogram: a report from the Pediatric Measurements Writing Group of the American Society of Echocardiography Pediatric and Congenital Heart Disease Council. *J Am Soc Echocardiogr*. 2010;23:465–495.
30. Pettersen MD, Du W, Skeens ME, Humes RA. Regression equations for calculation of z Scores of cardiac structures in a large cohort of healthy infants, children, and adolescents: an echocardiographic study. *J Am Soc Echocardiogr*. 2008;21:922–934.
31. Lang RM, Bierig M, Devereux RB, Flachskampf FA, Foster E, Pellikka PA, Picard MH, Roman MJ, Seward J, Shanewise JS, Solomon SD, Spencer KT, St John Sutton M, Stewart WJ. Recommendations for chamber quantification: a report from the American Society of Echocardiography's Guidelines and Standards Committee and the Chamber Quantification Writing Group, developed in conjunction with the European Association of Echocardiography, a branch of the European Society of Cardiology. *J Am Soc Echocardiogr*. 2005;18:1440–1463.
32. Rueb K, Mynard J, Liu R, Wake M, Vuillermin P, Ponsonby A-L, Zannino D, Burgner DP. Changes in carotid artery intima-media thickness during the cardiac cycle – a comparative study in early childhood, mid-childhood, and adulthood. *Vasa*. 2017;46:275–281.
33. Savitzky A, Golay M. Smoothing and differentiation of data by simplified least square procedures. *Anal Chem*. 1964;36:1627–1639.
34. Laurent S, Cockcroft J, Van Bortel L, Boutouyrie P, Giannattasio C, Hayoz D, Pannier B, Vlachopoulos C, Wilkinson I, Struijker-Boudier H. Expert consensus document on arterial stiffness: methodological issues and clinical applications. *Eur Heart J*. 2006;27:2588–2605.
35. Kowalski RR, Beare R, Mynard JP, Cheong JLY, Doyle LW, Smolich JJ, Cheung MMH. Increased aortic wave reflection contributes to higher systolic blood pressure in adolescents born preterm. *J Hypertens*. 2018;36:1514–1523.
36. Niki K, Sugawara M, Chang D, Harada A, Okada T, Sakai R, Uchida K, Tanaka R, Mumford CE. A new noninvasive measurement system for wave intensity: evaluation of carotid arterial wave intensity and reproducibility. *Heart Vessels*. 2002;17:12–21.
37. Ohte N, Narita H, Sugawara M, Niki K, Okada T, Harada A, Hayano J, Kimura G. Clinical usefulness of carotid arterial wave intensity in assessing left ventricular systolic and early diastolic performance. *Heart Vessels*. 2003;18:107–111.
38. Zambanini A, Cunningham SL, Parker KH, Khir AW, McG Thom SA, Hughes AD. Wave-energy patterns in carotid, brachial, and radial arteries: a noninvasive approach using wave-intensity analysis. *Am J Physiol Heart Circ Physiol*. 2005;289:H270–H276.
39. Watanabe H, Kawai M, Sibata T, Hara M, Furuhata H, Mochizuki S. Noninvasive measurement of aortic pressure waveform by ultrasound. *Heart Vessels*. 1998;13:79–86.
40. Harada A, Okada T, Niki K, Chang D, Sugawara M. On-line noninvasive one-point measurements of pulse wave velocity. *Heart Vessels*. 2002;17:61–68.
41. Kowalski R, Beare R, Willemet M, Alastruey J, Smolich JJ, Cheung MMH, Mynard JP. Robust and practical non-invasive estimation of local arterial wave speed and mean blood velocity waveforms. *Physiol Meas*. 2017;38:2081–2099.
42. Davies JE, Whinnett ZI, Francis DP, Manisty CH, Aguado-Sierra J, Willson K, Foale RA, Malik IS, Hughes AD, Parker KH, Mayet J. Evidence of a dominant backward-propagating "suction" wave responsible for diastolic coronary filling in humans, attenuated in left ventricular hypertrophy. *Circulation*. 2006;113:1768–1778.
43. Jones CJH, Sugawara M, Kondoh Y, Uchida K, Parker KH. Compression and expansion wavefront travel in canine ascending aortic flow: wave intensity analysis. *Heart Vessels*. 2002;16:91–98.
44. Penny DJ, Mynard JP, Smolich JJ. Aortic wave intensity analysis of ventricular-vascular interaction during incremental dobutamine infusion in adult sheep. *Am J Physiol Heart Circ Physiol*. 2008;294:H481–H489.
45. Mynard JP, Smolich JJ. Wave potential and the one-dimensional windkessel as a wave-based paradigm of diastolic arterial hemodynamics. *Am J Physiol Heart Circ Physiol*. 2014;307:H307–H318.
46. Xu J, Shiota T, Omoto R, Zhou X, Kyo S, Ishii M, Rice MJ, Sahn DJ. Intravascular ultrasound assessment of regional aortic wall stiffness, distensibility, and compliance in patients with coarctation of the aorta. *Am Heart J*. 1997;134:93–98.
47. Ou P, Celermajer DS, Jolivet O, Buyens F, Herment A, Sidi D, Bonnet D, Mousseaux E. Increased central aortic stiffness and left ventricular mass in normotensive young subjects after successful coarctation repair. *Am Heart J*. 2008;155:187–193.
48. De Divitiis M, Pilla C, Kattenhorn M, Zadinello M, Donald A, Leeson P, Wallace S, Redington A, Deanfield JE. Vascular dysfunction after repair of coarctation of the aorta: impact of Early Surgery. *Circulation*. 2001;104:I–165–I–170.
49. Ou P, Celermajer DS, Mousseaux E, Giron A, Aggoun Y, Szezepanski I, Sidi D, Bonnet D. Vascular remodeling after "successful" repair of coarctation: impact of aortic arch geometry. *J Am Coll Cardiol*. 2007;49:883–890.
50. Taelman L, Bols J, Degroote J, Muthurangu V, Panzer J, Vierendeels J, Segers P. Differential impact of local stiffening and narrowing on hemodynamics in repaired aortic coarctation: an FSI study. *Med Biol Eng Comput*. 2015;54:497–510.
51. van den Wijngaard JPHM, Siebes M, Westerhof BE. Comparison of arterial waves derived by classical wave separation and wave intensity analysis in a model of aortic coarctation. *Med Biol Eng Comput*. 2009;47:211–220.
52. Swan L, Kraidly M, Muhll IV, Collins P, Gatzoulis MA. Surveillance of cardiovascular risk in the normotensive patient with repaired aortic coarctation. *Int J Cardiol*. 2010;139:283–288.
53. Karamanoglu M, Feneley MP. Late systolic pressure augmentation: role of left ventricular outflow patterns. *Am J Physiol*. 1999;277:H481–H487.
54. O'Rourke MF, Pauca AL. Augmentation of the aortic and central arterial pressure waveform. *Blood Press Monit*. 2004;9:179–185.
55. Fok H, Guilcher A, Li Y, Brett S, Shah A, Clapp B, Chowienczyk P. Augmentation pressure is influenced by ventricular contractility/relaxation dynamics: novel mechanism of reduction of pulse pressure by nitrates. *Hypertension*. 2014;63:1050–1055.
56. van de Velde L, Eeftinck Schattenkerk DW, Venema PAHT, Best HJ, van den Bogaard B, Stok WJ, Westerhof BE, van den Born BJH. Myocardial preload alters central pressure augmentation through changes in the forward wave. *J Hypertens*. 2018;36:544–551.
57. Ou P, Celermajer DS, Raisky O, Jolivet O, Buyens F, Herment A, Sidi D, Bonnet D, Mousseaux E. Angular (Gothic) aortic arch leads to enhanced systolic wave reflection, central aortic stiffness, and increased left ventricular mass late after aortic coarctation repair: evaluation with magnetic resonance flow mapping. *J Thorac Cardiovasc Surg*. 2008;135:62–68.
58. Cuypers J, Leirgul E, Larsen TH, Berg A, Omdal TR, Greve G. Assessment of vascular reactivity in the peripheral and coronary arteries by cine 3T-magnetic resonance imaging in young normotensive adults after surgery for coarctation of the aorta. *Pediatr Cardiol*. 2012;34:661–669.
59. Balderrábano-Saucedo NA, Vizcaíno-Alarcón A, Reyes-de la Cruz L, Espinosa-Islas G, Arévalo-Salas A, Segura-Stanford B. Left ventricular function in children after successful repair of aortic coarctation. *Rev Esp Cardiol*. 2008;61:1126–1133.
60. Moskowitz WB, Schieken RM, Mosteller M, Bossano R. Altered systolic and diastolic function in children after "successful" repair of coarctation of the aorta. *Am Heart J*. 1990;120:103–109.
61. de Divitiis M, Pilla C, Kattenhorn M, Donald A, Zadinello M, Wallace S, Redington A, Deanfield J. Ambulatory blood pressure, left ventricular mass, and conduit artery function late after successful repair of coarctation of the aorta. *J Am Coll Cardiol*. 2003;41:2259–2265.